Article:
Zhang, M, Xu, C, Du, X et al. (2 more authors) (2017) Off-design performance of concentrated solar heat and coal double-source boiler power generation with thermocline energy storage. Applied Energy, 189. pp. 697-710. ISSN 0306-2619

https://doi.org/10.1016/j.apenergy.2016.12.095

Off-design performance ofconcentrated solar heat and coal double-source boilerpower generation with thermocline energy storage

Maolong Zhang[a,c],Chao Xu[a], XiaozeDu[a†], Muhammad Amjad[c,a], Dongsheng Wen[b,c†]

[a] *School of Energy, Power and Mechanical Engineering, North China Electric Power University, Beijing 102206, China*

[b]*School of Aeronautic Science and Engineering, Beihang University,Beijing 100191, PR China*

[c]*School of Chemical and Process Engineering, University of Leeds, Leeds LS2 9JT, UK*

Highlights

1.The off-design performance of a dual heat source powerunit (solar+coal)is studied.

2. A whole-system model is established and two integration schemes are studied.

3.. Coal consumption can be reduced by >9×10^4 ton/yrfor a 660 MW unit.

4. Annual solar efficiency can vary from 17.7 to 20.4% depending on the integration scheme.

5. Increasing heat storage volume decreases discharging efficiency.

6. Such a hybrid system is promising for future applications.

Abstract

Integration of solar thermal energy into a coal-fired power station is a promising technology for many coal-dependent countries. This work revealed the off-design performance of such a dual heat source boiler power generation from a system-level modelling approach. As an example study, heat from a solar power tower (SPT)was integrated into a 660 MW supercritical coal-firing power unit, and two integration schemes were considered. A system level analytical model was established that coupled the transient process of heliostat field with one-tank thermocline thermal energy storage,

†Corresponding author. Tel.: +86(10)61773923; Fax: +86(10)61773877.Email address: duxz@ncepu.edu.cn(X. Du); D.Wen@leeds.ac.uk (D. Wen)

and the off-design performance of such a hybrid system in one typical year was analyzed accordingly. The results showed that importance of the seasonal variation of direct normal insolation (DNI), thermal energy storage scheme and integration methodology. Both the quality of sunshine and the amount of sun flux influences the solar power efficiencyandan increase in the storage volume can decrease the discharging efficiency. Under the maximum capacity of DNI, increasing the storage capacity by 1h can improve the efficiency by 0.5-0.8%. For either integration scheme, the coal consumption can be economized at least9×10^4 ton per year. The maximum of solar efficiency for Scheme I, wheresolar energy is used to heat the superheat steam, reached 20.42%,which also came with a penalty of reduced lifetime for the SPT..

Keywords**:** concentrated solar heat and coal double-source boiler, supercritical power generation, system integration, off-design performance

Nomenclature

DNI direct normal insolation, W/m^2

MSHE molten-salt heat exchanger

SPT solar power tower

SAPG solar aided power generation

C_p specificheat capacity, $J/(kg\ ^{\circ}C)$

M mass flow rate, kg/s

N number

P power, MW

Q thermal load or thermal heat, kJ/kg–coal or W

T temperature, $^{\circ}C$

U heat transfer coefficient, $W/(K\cdot m^2)$

h enthalpy, kJ/kg

f optical factor

u velocity of salt

Greek symbols

η efficiency

ε porosity factor

ρ density, kg/m^3

Subscripts

ac actual

coal standard coal

dc designed coal

ex exchanger

f	furnace
helio	heliostat
in	inlet
ms	main steam
l	liquid salt
or	original
out	outlet
rec	receiver
reh	reheater
s	solid filler
sb	shading and blocking
std	standard
sol	solar
w	water

1. Introduction

With increasing concerns onCO_2 emission and fossil resource shortages, ,concentrated solar power (CSP) has become a promising technology to reshape our energy future [1,2].However, there are lots of technological and economic difficulties, including the temporal and seasonal fluctuation of solar flux, proper selection of energy storage system and itesintegration, and huge initial investment of a large scale CSP plant, which prevents its large scale application[3]. For many countries such as China, the major energy is supplied by coal [4],and the coal consumption rate for power generation has been decreased to the baseline by the usual system modification and optimization [5], which further limits the application of CSP alone.

The idea of integration of solar energy into a coal-fired power generationsystem has begun since 1970's [6-8], whichfocuses on replacingthe extracted steam from turbine by solar heating from parabolic trough (PT) collectors. The technology is also commonly known as thesolar aided power generation (SAPG).Severalinvestigationshave been conducted recently by Yang et al. [9-10] and Hu et al. [11-12]about the integration mechanism and the influenceof solar energy introduction. In terms of off-design performance, Hou et al. [13] and Peng et al. [14] did the analysis of the optimum solar field aperture and operation mode under differentdirect normal insolation (DNI) data, respectively.These studies indicated that SAPG wasa reasonable way for high efficiency utilization of solar energy and for effective reduction of CO_2emission in the coal-fired power generation.

As the operation temperature of solar power towers(SPT) is much higher than that of PT technology [15], it is expected that proper integration of solar heat from SPTwith the boiler of a coal fired power generating unit could achieve higher power efficiency than that of traditional SAPGtechnology. However, literature reviewshowed that there were little investigations about the complementation between the coal-fired power plant and SPT plant, despite of their high similarity in the operation structure and temperature range [16].

In our previous study concerning the performance of solar energy and coal dual heat source boiler [16], the possibility of introducing solar heat from SPT to a coal-fired boilerhas been verified. The performance of such a dual source boiler on the design point was discussed.However for any practical operation, various solar energy collector sub-systems, including the heliostat field, thermal receiver and molten salt heat exchanger (MSHE), as well as the variation of DNI, always resulting in off-design conditions. This could significantly affect the performance of the dual heat sources boiler and the overall power generating unit [17,18], for which little is known. This work aims to investigate such a problem by conducting a system level analysis to reveal the off-design operation characteristics of a whole power generating system with dual heat source boilers. The various influential parameters on the integration strategy of a model system including a 660 MW coal-fired power system and a 60 MW SPT are discussed, as well as the influence of thermal energy storage (TES) with one-tank thermocline technology [19,20].

2. Description and modeling on the system

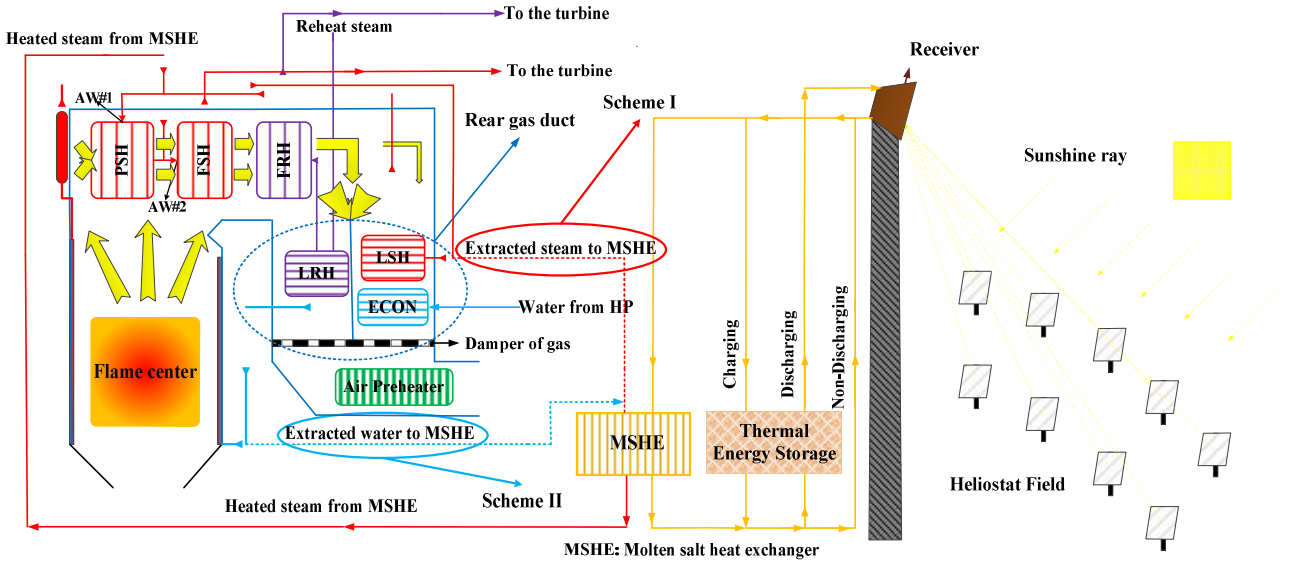

(a)Solar energy and coal dual heat source boiler. (AW: attemperation water; ECON; economizer; FSH: final superheater; FRH: final reheater; HP: high pressure heater; LSH: low-temperature

superheater; LRH: low-temperature reheater;MSHE: molten salt heat exchanger; PSH: platen superheater)

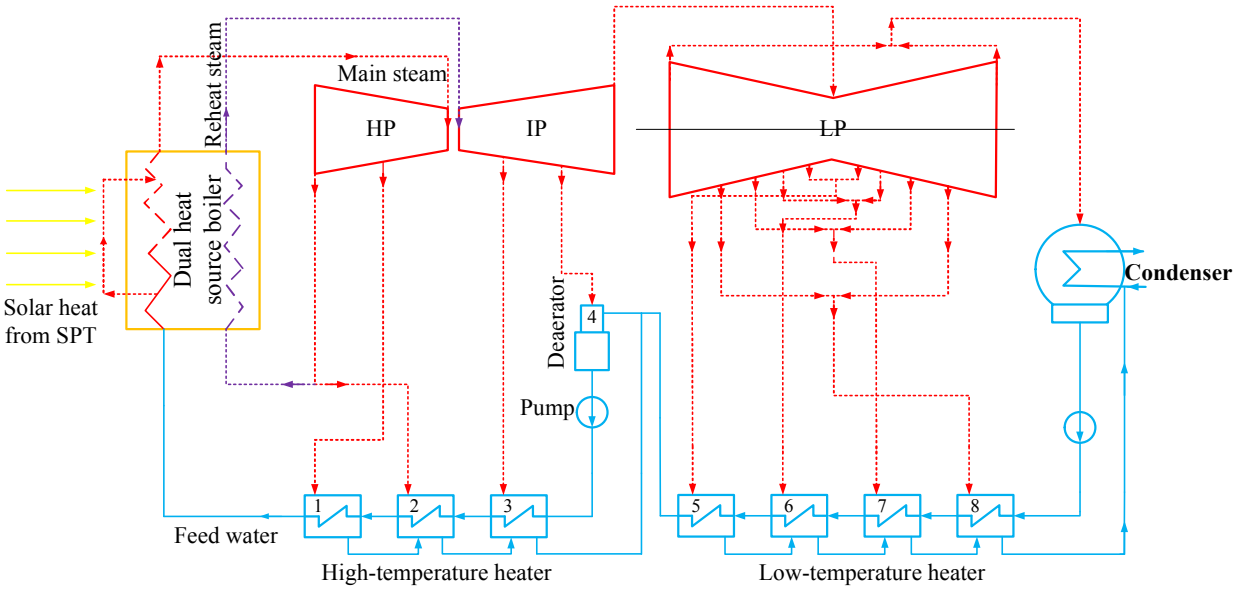

(b)Solar tower heat aided coal-fired power generation.

Fig. 1. Schematic diagram of the whole system combining SPT and coal-fired power generating units.

The components of the whole power generating system with dual heat source boilersare illustrated in Fig. 1. The heat transfer fluid in the thermal receiver of SPT is selected as liquid molten salt, which has excellent thermal properties both for heat transfer and thermal energy storage [21,22]. The solar heat is introducedto the boiler by the molten salt heat exchanger (MSHE). Because of the land restrictions in the coal-fired plant, the heliostat field is betterarranged north of the power plant, with the maximumthermal capacitybelow 90MW [23].Except the solar heat transferred to MSHE, the redundant heat can be also stored in the module of thermal energy storage (TES).According to theprevious analysis [16], two schemes of integration can be realized in the coupling system,targeting the superheat section and the evaporation sectionas indicated as Scheme I and II in Fig. 1(a), respectively. Fig. 1(b) illustrates the flow chart of steam or water in the

wholepower generating system, which consists of a three-cylinder turbine, two heat sources and eight extracted steam reheaters.

The system-level analytical model includes thetransient optical model of heliostat field utilizing the ray tracing method, the thermal model of receiver to calculate the mass flow rate of molten salt, the1-D transient simulation model of TES tank witha thermocline zone, the heat exchanger model transferring thermal energy between molten salt and water/steam, and at last the dual heat source boiler model with a turbine circle, which was built in the previous work [16].By combining all these sub-models, the performance of the hybrid system for two schemes of double-source boiler under DNI of one typical meteorological year is investigated. Since both the storage model and solar collector model are based on transient algorithm, they can be coupledtogether to make the steam turbine generating unit operating steadily, as described below. .

2.1 Solar collectors and receiver

For the solar power tower plant, the north heliostat field is made of thousands of heliostats while the corresponding receiver isin the shape of cavity [24]. The optical efficiency of the heliostat field,f_{op}, is divided into five parts: the cosine efficiency,f_{cos}, the blocking and shading efficiency,f_{sb}, the atmosphere attenuation efficiency,f_{att}, the interception efficiency f_{itp}, and the heliostat reflectivity f_{ref}, which can be calculated by the specific algorithm [17],

$$f_{op} = f_{cos} \cdot f_{itp} \cdot f_{att} \cdot f_{sb} \cdot f_{ref} \tag{1}$$

For the thermal receiver, the loss contains both the radiation loss through the open aperture and convection loss to the air [25].

The method to obtain the generation of heliostat field is derived from the CAMPO code that adopts radial staggered layout, while the calculation of efficiency is based on our previous work

[17]. The solar multiple is selected as 1.33, similar to PS10 [26]. To calculate the performance of the receiver, the thermal model from Li et al. [27],which considered forced convection, natural convection, conduction and radiation, is adopted in this work. To guarantee the stability of temperature at the outlet of receiver, the mass flow rate of the molten salt should be controlled and varied with the concentrated flux from the heliostat field,$Q_{\mathrm{rec,flux}}$, which can be acquired by,

$$M_{\mathrm{rec}}=Q_{\mathrm{rec,flux}}\cdot\eta_{\mathrm{rec}}/(C_{\mathrm{p,rec,out}}\cdot T_{\mathrm{rec,out}}-C_{\mathrm{p,rec,in}}\cdot T_{\mathrm{rec,in}}) \tag{2}$$

where$\eta_{\mathrm{rec,flux}}$ is the thermal efficiency ofreceiver, $T_{\mathrm{rec,out}}$ is the outlet temperature and $C_{\mathrm{p,rec,out}}$ is the thermal capacity of molten salt at the outlet of receiver.

2.2 Double heat source boiler

The operation temperature of molten salt in SPT plant is around 290-565℃ [21]. Two integration schemes with a 660MW supercritical boiler have been proposed [16]. The first one is from the inlet of low-temperature superheater (LSH) to the inlet of final superheater(FSH), and the other one is between the outlet of economizer (ECON) and the inlet of FSH. In both schemes, the working fluid of boiler is partly extracted and sent toMSHE, but the location of extraction is different. For Scheme I,the extracted working fluid is the superheated steam and for Scheme II, it is the subcooled water. It means that only the superheat part of the boiler is integrated in Scheme I, while the MSEHin Scheme II must include both evaporating and superheating sections. The detail of the integrations can be found in theliterature[16].

Taking both steam flow rate on the inlet/outlet of the boiler and the flux ofsolar heat into consideration, the coal consumption rateof the boiler can be obtained by,:

$$B_{\mathrm{dc}}\cdot Q_{\mathrm{coal}}=\sum_{i=1}^{\mathrm{n}}M_{\mathrm{ms},i}/3.6\times(h_{\mathrm{ms,out},i}-h_{\mathrm{ms,in},i})+M_{\mathrm{reh}}/3.6\times(h_{\mathrm{reh,out}}-h_{\mathrm{reh,in}}) \tag{3}$$

whereB_{dc}in kg/s is the consumption rate of designed coal, Q_{coal}in kJ/kg is calorific value of designed

coal, and$M_{\mathrm{ms},i}$ andM_{reh}in t/h are mass flow rate of main steam in the i^{th} high pressure heat exchanger and reheat steam from the high pressure turbine cylinder, respectively.

The saved standard coal consumption rate then can be calculated by,

$$\Delta B_{\mathrm{std}}=\frac{Q_{\mathrm{sol}}\times 3600}{660\times 10^{3}}\cdot\frac{1}{Q_{\mathrm{std}}} \tag{4}$$

whereQ_{std}in kJ/kg is calorific value of standard coal.

As the most concerned parameter, solar power efficiency,η_{sol},can be calculated by,

$$\eta_{\mathrm{sol}}=\frac{P_{\mathrm{sol}}}{Q_{\mathrm{input}}}*100 \tag{5}$$

whereP_{sol} is the power generated by the solar heat and $Q_{\mathrm{input}}$is the solar flux injected to the heliostat field, the value of which can be obtained by,

$$Q_{\mathrm{input}}=\mathrm{DNI}\cdot A_{\mathrm{helio}}\cdot N_{\mathrm{helio}}=Q_{\mathrm{rec\_flux}}/\eta_{\mathrm{op}} \tag{6}$$

whereA_{helio} is the area of single heliostat and N_{helio} is the number of heliostat in the field.

As a result, η_{sol} includes not only the thermal power generation efficiency in the turbine and the storage/heat exchange efficiency, but also the optical efficiency of heliostat field and the thermal efficiency of receiver.

2.3 One-tank thermal energy storage

Toadjust the fluctuation of sunlight in the day time and increase the stability of the complementation, thethermal energy storage unit (TES)filled up with molten salt is necessary, as shown in Fig. 1(a).

According to the phase of storage medium, the thermal storage technologies can be divided into sensible storage, phase change storage and thermal chemical storage, of which two-tank sensible storage technology is applied in most of the commercial solar plants [29]. However, compared to two-tank storage, the one-tank thermocline TES can save 20-37% cost according to some researches

[29,30].The simulation of the thermocline tank is taken based on a 1-D model considering mass and energy balance in a single unit, sothe equation for the velocity of molten salt in the tank can be calculated as follows [31]:

$$u_x = \frac{\varepsilon \cdot \rho_{x,\mathrm{l}} \cdot C_{\mathrm{p},x,\mathrm{l}} + (1-\varepsilon) \cdot \rho_{\mathrm{s}} \cdot C_{\mathrm{p,s}}}{\varepsilon \cdot \rho_{\mathrm{in,l}} \cdot C_{\mathrm{p,in,l}} + (1-\varepsilon) \cdot \rho_{\mathrm{s}} \cdot C_{\mathrm{p,s}}} \cdot \frac{\rho_{\mathrm{in,l}}}{\rho_{x,\mathrm{l}}} \cdot u_{\mathrm{in}} \tag{7}$$

where$u$ is the velocity of liquid salt, ρ is the density, ε is porosity of packed-bed area, andthe subscripts, x, l, and s mean the inlet, point x, liquid salt and solid fillerrespectively.

Byusing this equation, the solver of N-S equation for fluid field can be omitted to simplify the calculation. The accuracy of this simplified model has been validated by other researchers [31], and the time step for the CFD simulation of packed-bed is set as 5s [20,22].

The other detailsabout the physical properties and heat transfer models in the thermocline tank can be referred to our previous work [20,22], which also have been validated by the experimental data.

2.4Molten salt heat exchanger

In Scheme I, the molten salt exchanger just transports heat to the superheat steam, like the superheater in Solar Two [21]. Therefore, the design data of exchanger in Solar Two can be used in this part. The heat transfer coefficient of superheaterwith the mass flow rate of salt or steam can be obtained based on the following equation [18],

$$\frac{U_{\mathrm{ac}}}{U_{\mathrm{or}}} = \left(\frac{M_{\mathrm{ex,l,ac}}}{M_{\mathrm{ex,l,or}}} \right)^{0.8} \cdot \left(\frac{M_{\mathrm{ex,w,ac}}}{M_{\mathrm{ex,w,or}}} \right)^{0.8} \cdot \left(\frac{M_{\mathrm{ex,l,or}} + M_{\mathrm{ex,w,or}}}{M_{\mathrm{ex,l,ac}} + M_{\mathrm{ex,w,ac}}} \right)^{0.8} \tag{8}$$

where$U$ is the heat transfer coefficient, ex and w respectively mean heat exchanger and water. This equation can also be deduced from Dittus-Boelter equation [32] by omitting the change of physical properties.

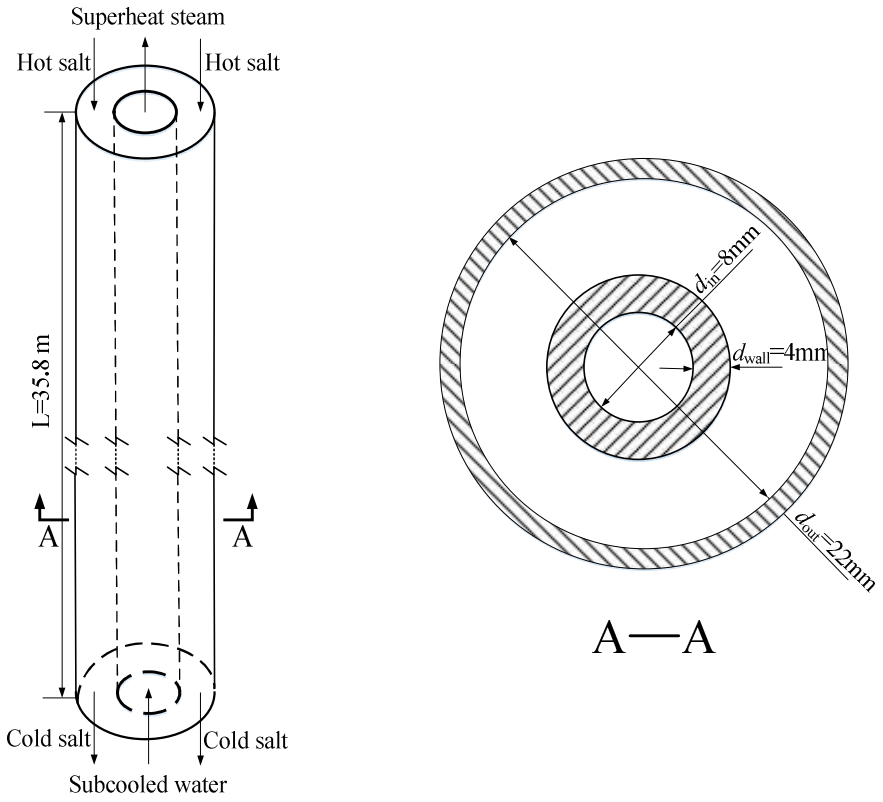

Fig. 2. Schematic diagram of the heat exchanger in Scheme II.

As the MSEH in Scheme II contains both evaporation and superheating sections of supercritical water/steam, the design data of Solar Two cannot be used. Fig. 2 shows that the heat exchanger can be changed to annular shape [33,34]including both evaporation and superheat sections with consideration of the instability of supercritical water during evaporation. For the present 660MW double source supercritical boiler, the total length of one single annual tube is 35.8 m.

The Nusselt number of the molten saltside can be obtained by [32],

$$Nu_{\mathrm{l}}=0.023\cdot Re_{\mathrm{l}}^{0.8}\cdot Pr_{\mathrm{l}}^{0.4} \tag{9}$$

and thatof the supercritical water/steam side isobtained by [35],

$$Nu_{\mathrm{w}}=0.0061\cdot Re_{\mathrm{b}}^{0.904}\cdot Pr_{b}^{0.684}\cdot\left(\frac{\rho_{\mathrm{wall}}}{\rho_{\mathrm{b}}}\right)^{0.564} \tag{10}$$

whereRe_{b} and Pr_{b} are respectively Reynolds number and Prandtl number of the bulk stream in the

tube. And ρ_{wall} is the density of water or steam at the wall temperature.

As shown in Fig. 2, the molten salt flows from upside to underside while the water/steam flows in the reverse direction. As the physical properties of supercritical water/steam change drastically with the temperature, the whole tube is divided into small sections along the flow direction during calculation. The parameters of medium at the outlet of formersection can be taken as the input variables to calculate the laterone.

2.5 Integration of the whole system

To emphasize the comparison and simplify the calculation, two assumptions are adopted in the system integration.

(1) Based on the policy support and environment care the integrated plant is assumed to be generating power on rated load all the time if the SPT section operates normally.

(2) For different DNI input and storage volume, the data of collector in SPT plant, including field shape, latitude location and receiver parameters,arekept as identical.

2.5.1 Heliostat field, receiver and one-tank packed-bed thermal energy storage

For the presentdouble heat source 660MW boiler, if the solar heat of input exceed about 90MW, the quality of steam at the outlet of boiler may not meet the need of rated condition [16]. In consideration of the safety allowance and the difference between the theoretical model and reality, the rated amount of solar heat to the coal-fired unit can beensured as 60MW. On such a basis, the models of heliostat field and thermal receiver can also be designed out, as well as the molten salt heat exchanger. The data about the size of heliostat and cavity receiver can refer to PS10 [26].It should be noticed that the design value of DNI and time point for heliostat field are respectively selected as 900 W/m^2 and the midday in thespring equinox.

In terms of thermocline storage, the design method can be found in [36] whilethe previous research [30] showed that on account of the operation characteristics of thermocline tank, 40%overdesign of the tank volume is necessary.Apart from that, to bear the gravity of the fillers the height of the tank should not exceed 11.89m. In another system-level research about the SPT plant with molten salt [31], the minimum of 2h storage was suggested for the stable performance in the daytime. In the present work, to discuss the influence of storage volume on the performance of whole system, three scales of thermocline tanks have been designed, which are $3\times60MWh_t$, $4\times60MWh_t$ and $5\times60MWh_t$, respectively.

2.5.2 The operation logic of whole system

Fig. 3 illustrates how the mathematical model of whole system operates logically. The time interval for the calculation of the solar flux is set as 15 minutes. In the daytime, when the elevation angle of sun surpasses 15˚, the concentration of solar flux starts. . At the beginning, all the heat from the receiver flows to the packed-bed TEStank. After the stored energy reaching 2h discharge amount, the integration of solar heat flux with coal-fired boiler starts to work. As the coal fired power plant is assumed to keep designed condition through the whole year, the solar heat from SPT to the boiler is also kept almost constant of 60MW. Therefore, the mass flow rate of molten salt at the outlet of receiver has a rated value, M_{rate}. When M_{rec} is over M_{rate}, the redundant heat from the receiver is charged into the TES tank. On the contrary, when M_{rec} is less than M_{rate}, the TES discharges supplementary energy to the MSHE.

During the charging process, if the outlet temperature of storage tank exceeds the downside threshold temperature, $t_{down,thr}$, the redundant heat has to be discarded. By contrast, during the discharging process, if the outlet temperature of the tank lags behind the upside threshold temperature, $t_{up,thr}$, the thermocline have no heat to supply the power generation unit. The details

of data in the integration system are shown in table 1.

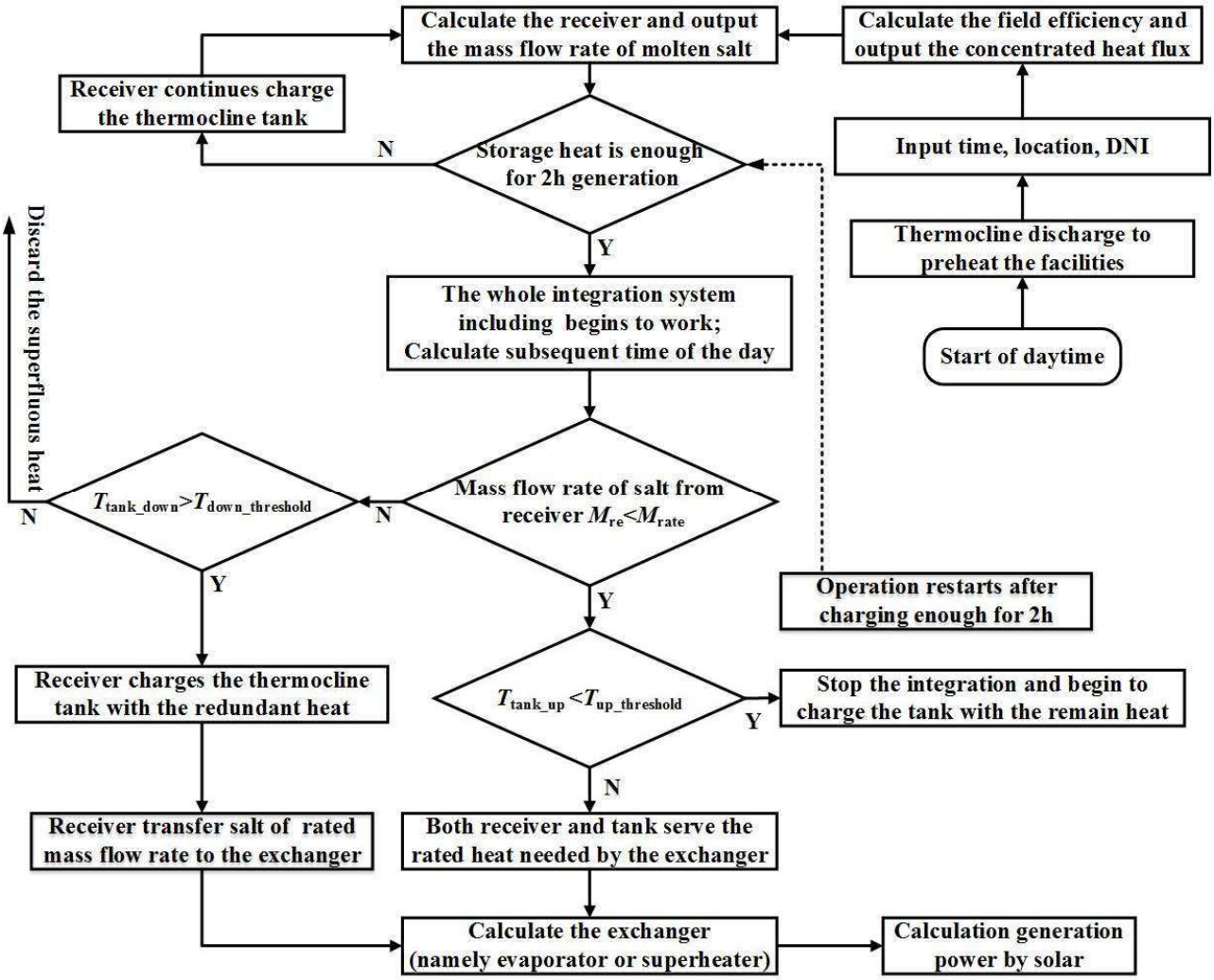

Fig. 3. The logic flow chart of whole system.

Table 1. The operation details of two integration schemes.

	Scheme I	Scheme II
Temperature range of salt	452-575℃	335-565℃
Temperature range of integration water	422-545℃	310-540℃
Integration sections of boiler	Superheating	Evaporation and Superheating
Heat exchanger type	Schell and tube	Annular

Upside threshold of tank, $t_{up,thr}$℃	568.5	553.5
Downside threshold of tank, $t_{down,thr}$℃	457	360
Porosity of packed-bed, ε	0.22	0.22

3. Results and discussions

For any practical operation, all the stored energy must be drained out to recover the thermocline tank to the original stateat the end of each monthto keep the characteristics of thermocline zone and guarantee the normal operation of TES. Therefore, the following results are discussed .

3.1 Different solar flux and SPT contribution

To reveal the influence of different DNI values on the performance of integration system, three DNI values (high, medium, low) of a typical meteorological year (TMY), as shown in Fig. 4(a), are adopted, which come from Western America, Southern Spain and Northwest China, respectively [37]. Since the weather data are recorded hourly, the value of DNI for each 15 minutes must be recalculated by the interpolation method, with the consideration of the difference between the solar time and local time.In the real operation of SPT, the day time usually means a minimum of 15° of sun elevation over the horizon line, so the sunshine in Fig. 4(a) with elevation angle less than 15°has to be filtered[38]. The annual DNI distribution after recalculationwithin day time is shown in Fig. 4(b), where it can be found that the difference between annual totalsolar insolation density of the first type and those of the other two types is reduced. For example, the annual insolation density of high DNI is decreased from 2014.1 kWh/m^2/year to 1624.5 kWh/m^2/year while the density of Medium DNI is only changed from 1737.7 kWh/m^2/year to 1506.3 kWh/m^2/year.

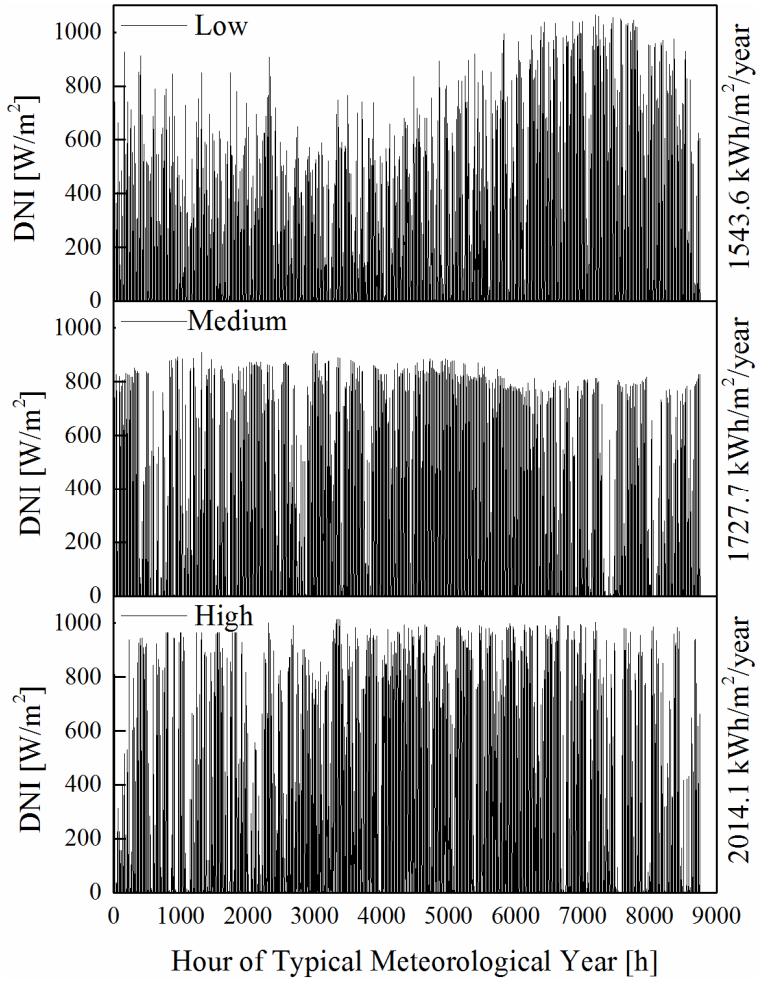

(a) Original distribution.

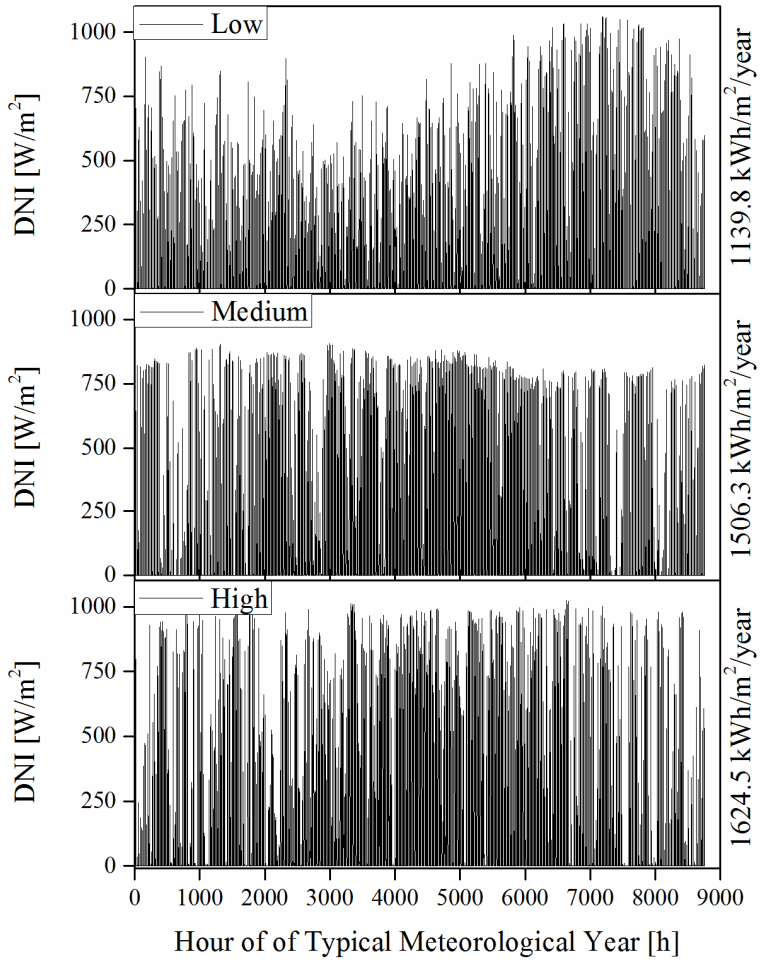

(b) Expelling DNI below 15˚elevation.

Fig. 4. Three typical annual DNI distributionsof a typical meteorological year.

The method to define solar contribution to the whole system is very important in the system level analysis. Since the heat from SPT was integrated to the boiler instead of the turbine, the general method by analyzing the turbine model can't be used in this part. One evaluating model based on the T-S diagram of whole coal-fired plant has been introduced for the dual heat source boiler previously [16]. The enthalpy and entropy values at the integration points can be obtained through the designed condition and by calculating the counterpart heat releasing sections in T-S figure, as well as the power generated by the solar heat .

3.2 PerformanceofScheme I

3.2.1 Solar efficiency,η_{sol},and economized coal consumption,ΔB_{std}

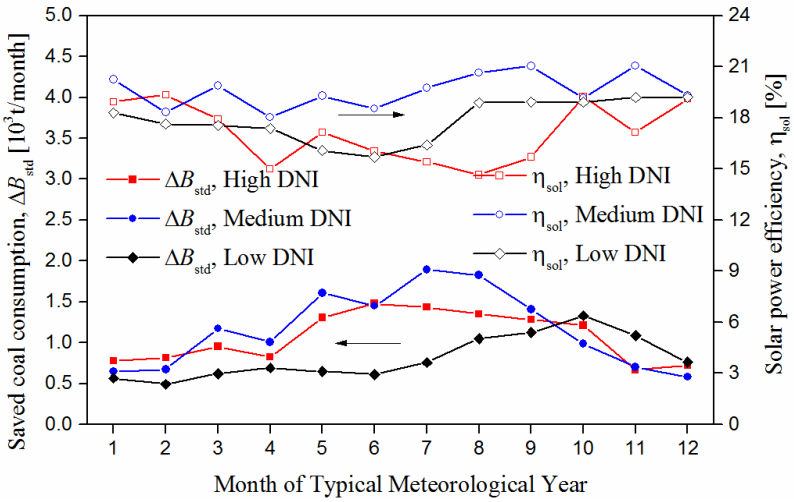

(a) 3h storage volume

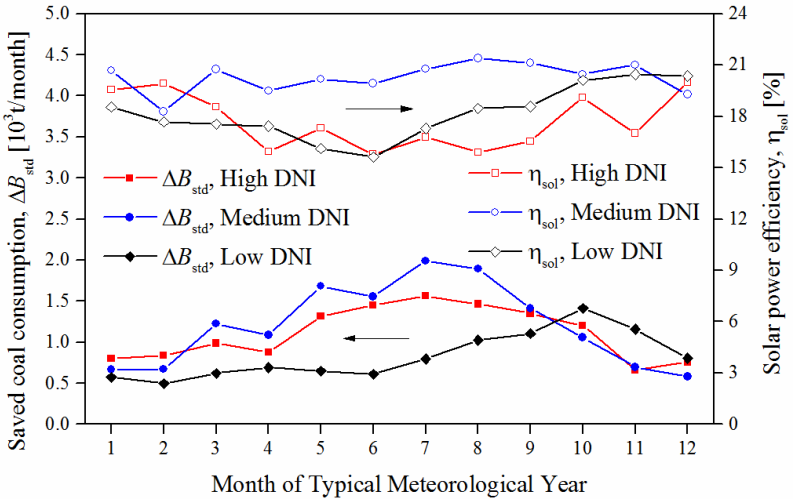

(b) 4h storage volume

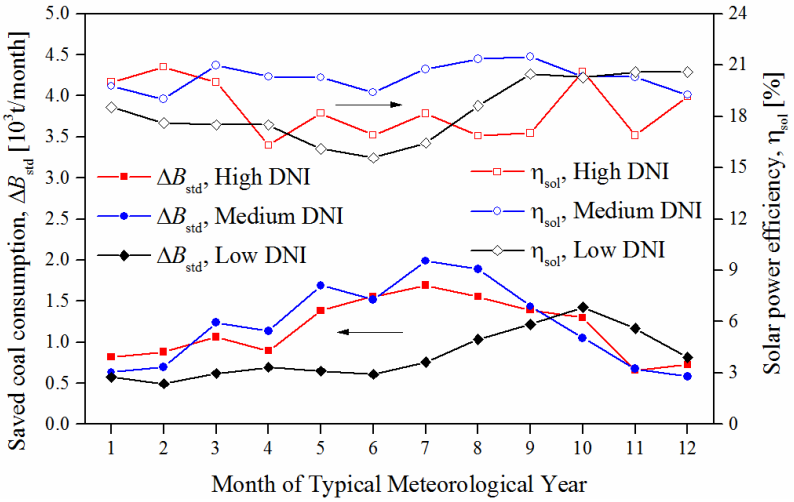

(c) 5h storage volume

Fig. 5. Variation of $\Delta B_{std}$and η_{sol} in one year with different storage volumes.

Fig. 5 shows the variation of solar efficiency in one year under three types of DNI distribution and three volumes of thermal energy storage.It is surprising that the efficiency of the medium DNI,instead thatof the high DNI,is always the highest. Even compared with low DNI input, the advantage of high DNI just appears in a short time.The reason can be attributed to the quality of sunshine. It can be found from Fig. 4 that the sun time is more focused around noon in the medium DNI. As a contrast, the sunrise time of high DNI appears earlier than the other two types caused by the higher latitude. Additionally, in many days of high DNI year the sunshine just appears in the morning or afternoon because of the weather change, which cannot be taken as effective day time for the sun elevation over the horizon may be lower than 15°.

Nevertheless, the quantity of DNI can still have significant influences. By comparing Fig.5(a), (b) and (c), it can be found thatthe solar efficiency,η_{sol},can increase with the TES volume. Under 3h storage, the annual efficiency of three DNI distributions are respectively 17.05%, 19.75% and17.75% ; while under 5h storage, these figures change into 18.16%, 20.42% and 18.58%. Because high DNI distribution can make better use of TES volume, the efficiency drawbackunder high DNI is mitigated comparing the other two DNI distributions.It can be deduced that the superiority of high DNI can be enhanced for larger storage volume.

As defined in Eq.(4), another key parameter of the integrated system with solar heat and coal is the quantity of saved standard coal consumption, ΔB_{std}, which is also shown in Fig.5. The variation of ΔB_{std} is much similar to that of DNI quantity. The TESvolume has also a small influence.

The annual performances of the integrated system with different TES volumesare summarized in Table2.Because of the efficiency advantage, the medium DNI distribution can save the

largestamount of standard coal. For the worst DNI distribution, it canstill save nearly 10^4ton coal per year, which indicates the promising potential of such a hybrid system.

Table 2. Annual performance of the integration systemsof Scheme I.

Storage volume	η_{sol}, % High DNI	η_{sol}, % Medium DNI	η_{sol}, % Low DNI	ΔB_{std}, 10^3 t High DNI	ΔB_{std}, 10^3 t Medium DNI	ΔB_{std}, 10^3 t Low DNI
3h	16.73	19.62	18.00	12.81	13.96	9.74
4h	17.33	20.40	18.38	13.27	14.52	9.95
5h	18.16	20.42	18.58	13.92	14.53	10.06

In Table 2, in comparison to the obvious efficiency improvement withincreasingTES volumeunderhigh DNI distribution, the efficiency variation of medium or low distribution is very slight when the storage volume changes from 4h to 5h. The phenomena can be explained by Fig. 6, which shows the change of discard thermal energy under different designs.For the medium distribution, when the storage volume increases to 5h, the discard solar heat by the system has fallen to zero. Therefore, further increasing the storage volumecannot improve the solar performance any more. As shown in Fig. 6, since the blue line ofmedium DNI is very close to the red line, the efficiency difference between 4h and 5h storage in Table 2 is just 0.02%.

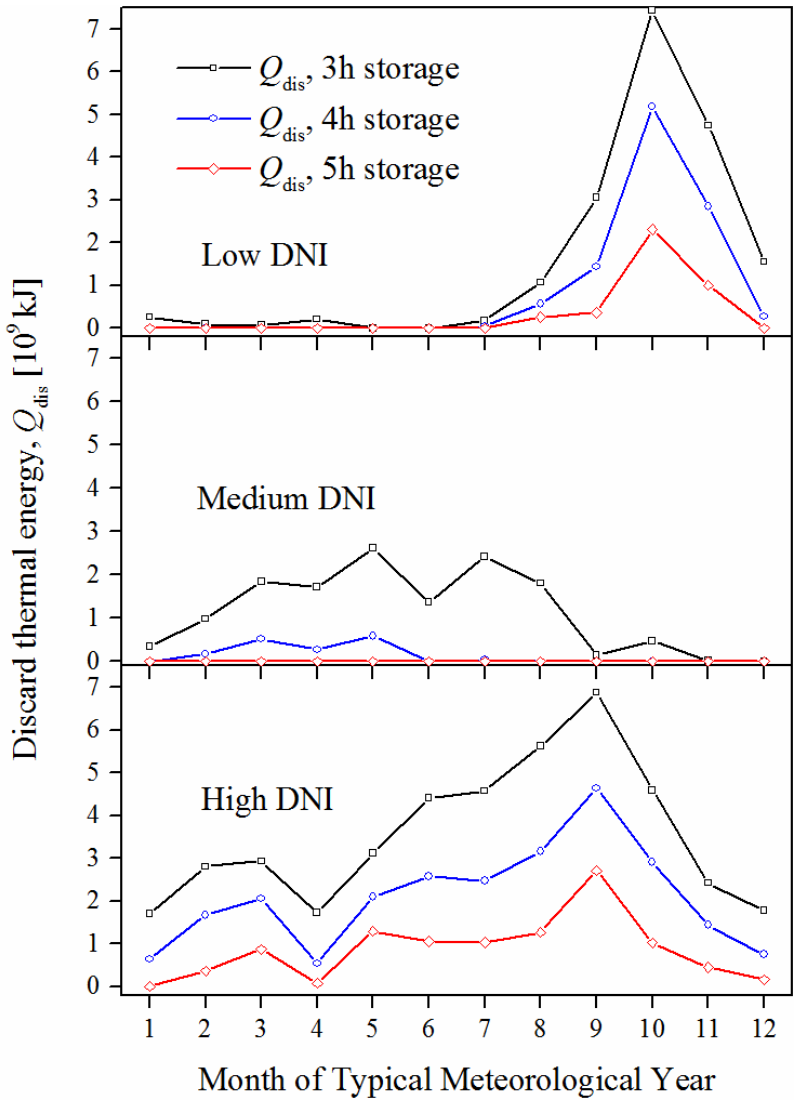

Fig. 6 Discard thermal energy during the whole year operation of Scheme I

3.2.2 Influence of storage volume on $\eta_{\text{discharge}}$and η_{TPG}

The discharge efficiency,$\eta_{\text{discharge}}$, and the thermal power efficiency,η_{TPG}, are respectively defined as,

$$\eta_{\text{discharge}}=\frac{Q_{\text{discharge}}}{Q_{\text{charge}}}\cdot 100\% \tag{11}$$

$$\eta_{\text{TPG}}=\frac{P_{\text{sol}}}{Q_{rec\_flux}\cdot\eta_{\text{rec}}}\cdot 100\% \tag{12}$$

where$Q_{\text{discharge}}$and $Q_{\text{discharge}}$ are respectively the discharged or charged thermal energy during the

same period.

As mentioned before, the tanks with different TES volume have the same tank height but different diameters, based on which the comparison for discharge efficiency,$\eta_{discharge}$, and thermal power efficiency,η_{TPG}, is shown in Fig. 7. In terms of η_{TPG}, although the difference is tiny, increasing the TES volume will reduce the thermal power efficiency.The reason can attribute to that the temperature of molten salt flowing outside the packed bed is not always at the rated temperatureduring the discharging process, especially considering the heat transfer temperature difference. With the stored energy reduced, the temperature also falls to the limited value. On the basis of Carnot's theorem, $\eta_{TPG}$is reduced as well.In addition, the thickness of thermocline also affects the results, which will be discussed below.

The discharge efficiency,$\eta_{discharge}$,can be determined by the thickness of thermocline and the threshold value at the top of the tank [20]. The larger the thermocline thickness, the smaller the temperature gradient is. When the outlet temperature reaches the threshold value during the discharging process, the packed-bed tank with a smaller temperature gradient has more unusable stored energy. Since the latter value is fixed, the difference of $\eta_{discharge}$ is mainly caused by the different thickness of thethermocline, as the velocity of fluid is decided by the diameter of tank. Unlike the conclusions from Yang and Garimella [36],of which the thickness increased with Re number and velocity, Fig. 7 shows that the discharging efficiency or the thermocline thickness can be decreasedwith a larger tank diameter and a smaller velocity.

To explain such a difference, the tank model of Xu [20] from the experimental data is employed, and 2-D simulation model of Xu is also adopted. By selecting the center point in the discharging process to compare like Yang and Garimella [36], the results are shown in Fig. 8(a), where the thickness for Re=10 is indeed wider than that that of Re=1, similar to Ref. [36]. However, it can be also found that when Re number is further decreasedto 0.1, the thickness of

thermocline increases much more as well. The reason is that despite the conductivity of molten salt keeping nearly constant, the convective heat transfer has been weakened too much because of the slowed speed, shown in Fig. 8(b). Therefore, the conduction in the molten salt plays the key role in the occasion and the thickness of thermocline can be widened. In other word, slower speed can decrease the temperature difference between the salt and fillers and improve the heat transfer efficiency, shown in Fig. 8(b). However further reduction of the thermocline thickness is not practical, because the mass flow rate in the storage tank of SPT always changes within one year off-design operation.

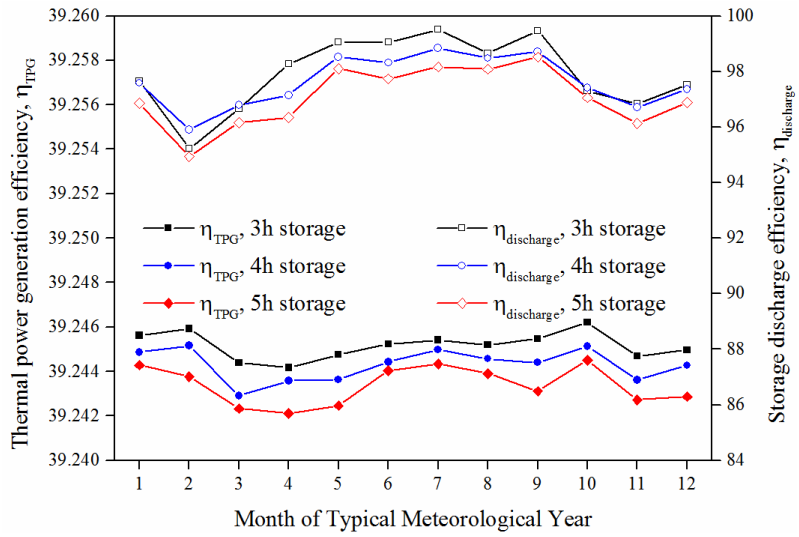

(a) High DNI

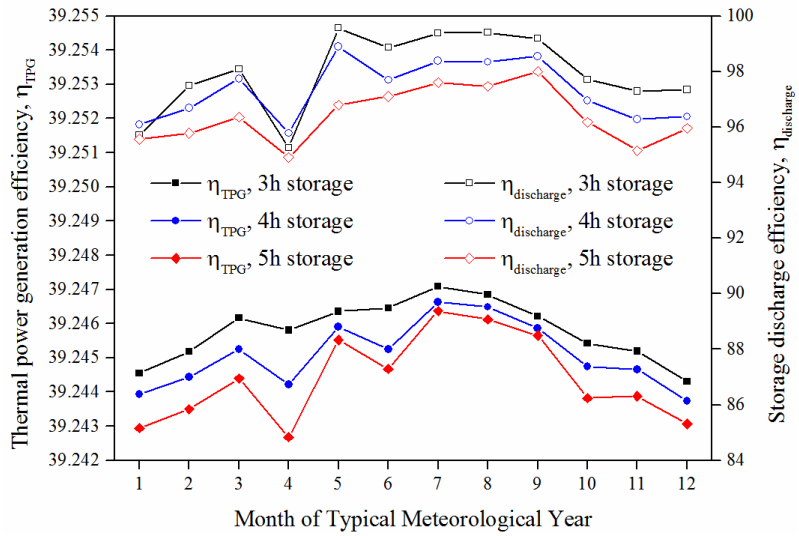

(b) Medium DNI

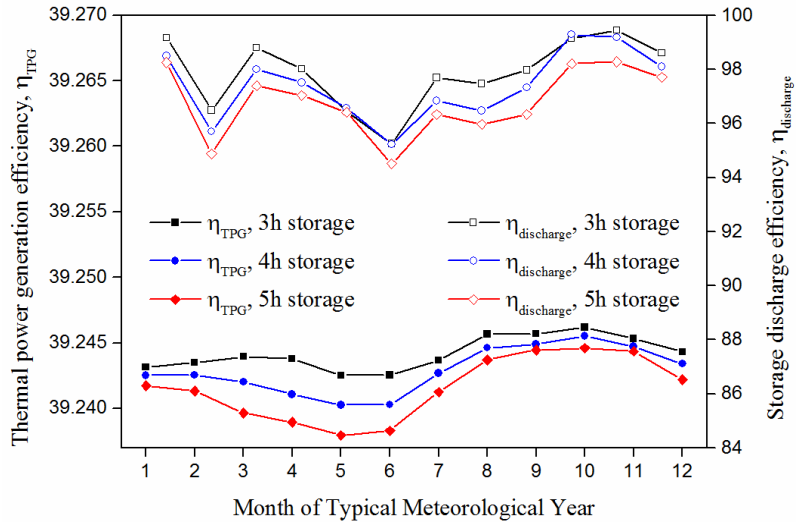

(c) Low DNI

Fig. 7 Variation of $\eta_{TPG}$and $\eta_{discharge}$ in one year under different storage volume.

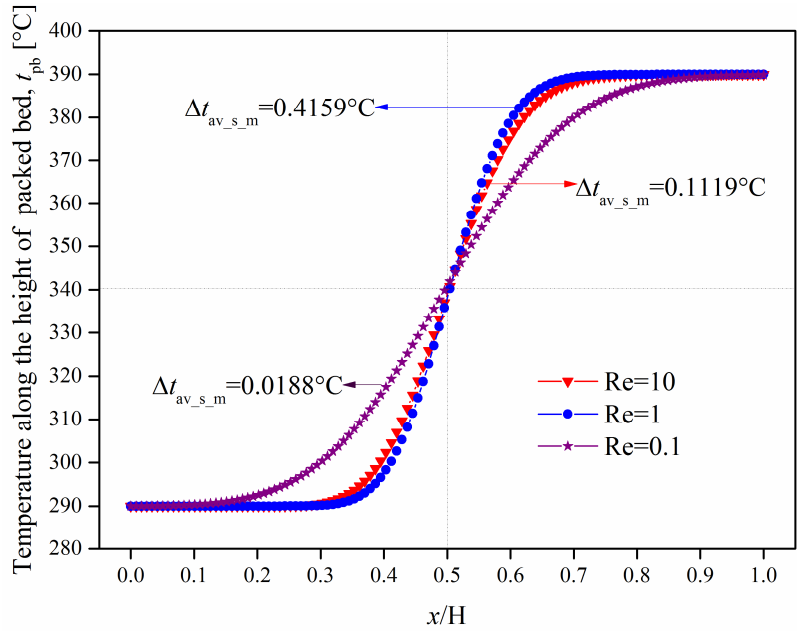

(a) Temperature profiles and average temperature difference between salt and fillers

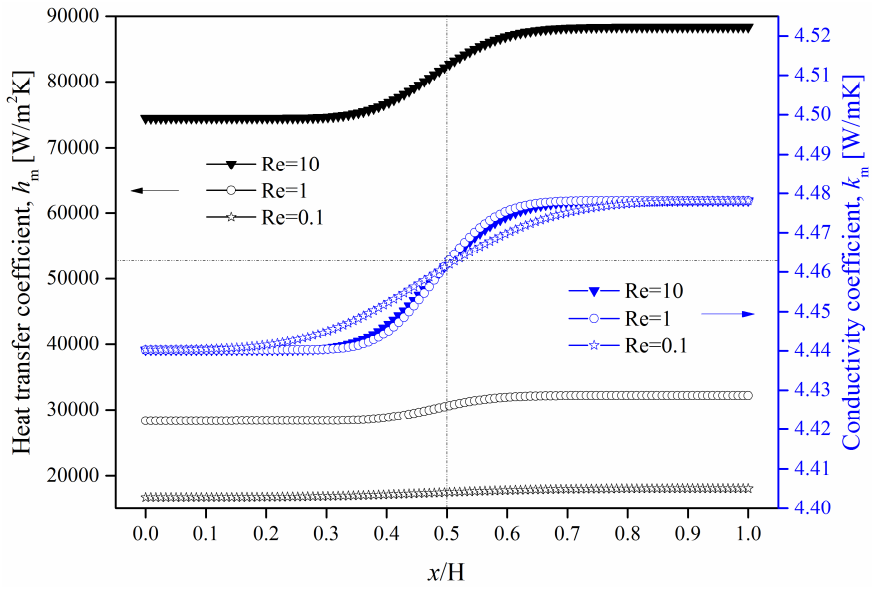

(b) Conductivity and heat transfer coefficient

Fig. 8 Comparisons of temperature profiles and heat transfer coefficient when Re number is 0.1, 1 and 10.

3.3Performance of Scheme II

Because the system of Scheme II is similar to that of Scheme I except the temperature range of

integration, most conclusions in Scheme I are applicable in Scheme II. . Fig. 9shows the variations of$\Delta B_{std}$and η_{sol} in Scheme II under three types of DNI flux with TES volume of 3×60MWh$_t$. The same conclusion can be obtained that Medium DNI behaves better than the other two types, no matter in the solar power efficiency or the saved coal consumption.For saved coal consumption ΔB_{std}, it is seen that the trend of Scheme II is still similar to that of Scheme I. However, since all the calculating equations about coal consumption are on the basis of the first thermodynamic law, the apparent difference in regard to ΔB_{std} between two schemes cannot be found.

Regarding to the annual solar power efficiency shown in Table 3, the efficiency of medium DNI is 17.33% while the efficiencies of high and low DNI are respectively 14.77% and 15.86%. Compared with the outcomes of Scheme I, the efficiency advantages of medium DNI and low DNI over high DNI have been magnified, which suggests that the advantage of optical efficiency for heliostat field can play a more important role in a lower integration temperature range. The reason is mainly about the operation of thermal receiver. When the temperature range becomes higher, the least demand for concentrated heat flux from heliostats is increased , leading to a reduced working time of heliostat field . When the integration temperature range decreases from Scheme I to Scheme II, the heliostat field can start earlier and stop later. As a result, the drawback of high DNI is magnified in Scheme II.

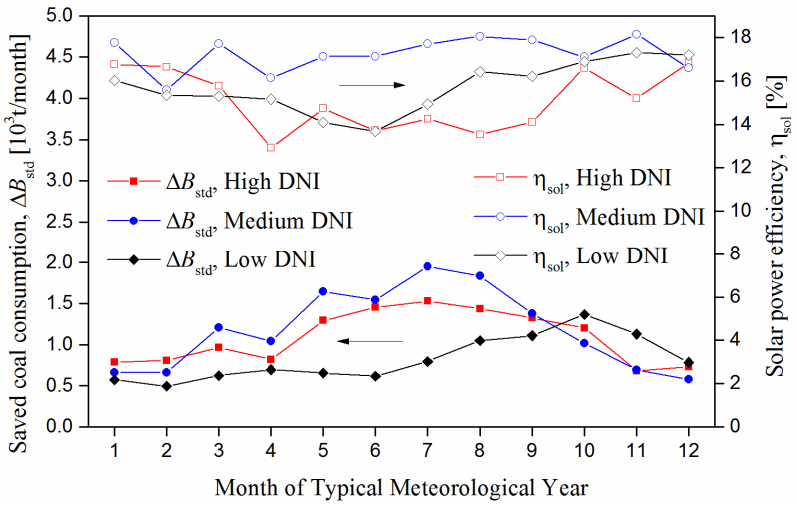

Fig. 9. Variations of ΔB_{std} and η_{sol}in one year under different DNI with 3h TES.

Table 3. Results of comparisons between Scheme I and Scheme II

System type	η_{sol}, %	$\eta_{discharge}$, %	η_{col}, %	P_{sol}, GWh	t_{sol}, h	t_{col}, h
Scheme I (Medium, 5h)	20.42	97.44	55.75	43.46	1852	1539
Scheme II (Medium, 5h)	17.68	97.74	56.14	37.70	1854	1540

The effects of TES volume in Scheme II on thermal power efficiency and storage discharge efficiency are also similar to that in Scheme I . For simplicity, only the results of Medium DNI with three types of TES volume are shown in Fig. 10.The average solar power efficiency η_{sol} of one whole year becomes 17.67% and 17.68% when the TES volume increases to 4×60MWh_t and 5×60Mh_t, respectively.

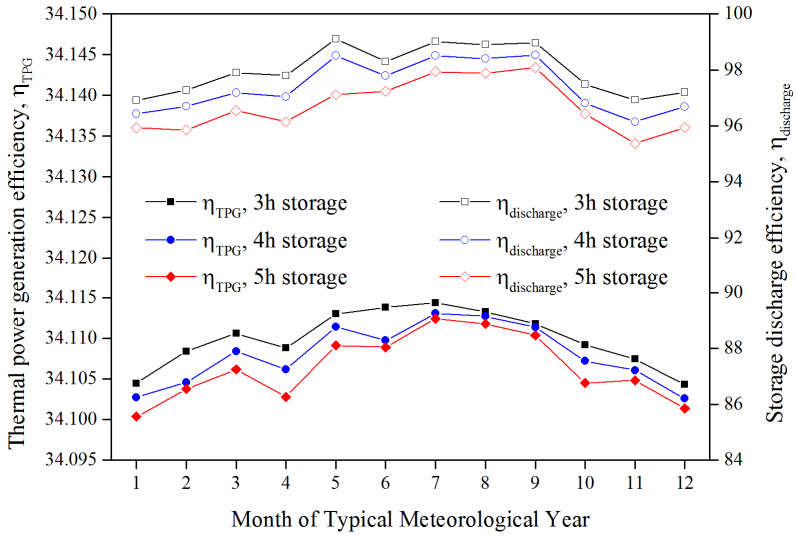

Fig. 10. Variations ofη_{TPG} and $\eta_{\mathrm{discharge}}$in one year with TESvolume under medium DNI.

3.4 Performance comparisons between Scheme I and Scheme II

Scheme I has a higher temperature range than Scheme II, therefore it can generate much more electric power under the same solar input. However, since the operation of solar receiver and thermocline is also affected by the temperature range, the power may not be accuratein proportion to the value of η_{TPG}. Table 3 compares several evaluation items of Scheme I and Scheme II where the DNI type is set as medium and storage volume, 5×60MWh$_t$.

From Table 3, it can be found that the annual solar power efficiency of Scheme I is about 2.74% higher than that of Scheme II while the difference in terms of the annual discharge efficiency is merely 0.3%. This suggests that for a given height of packed-bed tank, the temperature range just has a limited influence on the discharge efficiency of thermocline storageat the large system level.

For the solar power time mentioned inScheme II, both the solar power time, t_{sol}, and the collector operation time, t_{col}, are longer than those in Scheme I. Even for the efficiency of solar collector η_{col}, the advantage of Scheme II is nearly 0.39%, which is the result of the receiver

efficiency change. In the thermal receiver of Scheme I, the temperature range is higher, so the radiation loss and convection loss of receiver are also more than those in Scheme II. Therefore, the efficiency of the receiver is lower as well as the efficiency of solar collector, η_{col}.

4. Conclusions

As the solar input always fluctuates around the design values, the performance of whole system, especially for the CSP part, deviates from the designed point. In order to reveal the off-design performance of a dual heat source boiler power generation, a system-level analytical model was established, which coupled the transient process of heliostat field with one-tank thermocline thermal energy storage. Take a case study of a 660MW supercritical coal-fired power system, the annual performancewith two kinds of dual heat source boilerwas obtained and compared .The following conclusions can be acquired.

(1) In terms of solar input, both the quality and the quantity have influences on the annual performance of system,of which the former is more relative to the solar power efficiency and the latter plays a more important role on the amount of saved coal . The saved coal is sensitive tothe solar insolation density while the solar power efficiency has no obvious connection with the DNI value.

(2)The solar power efficiency under various DNI can beimproved by increasing the thermal energy storage volume, which however also results in decreased values for the discharge efficiency and thermal power efficiencybecause of the off-design operation.

(3) For a whole year operation of the double heat source power generationsystem, the solar power efficiency in the best annual performance of superheat schemecan be as high as 20.42% andthe saved coal consumption can be more than 10^4 ton per year for a 660MW supercritical power generating unit.

(4) Because of the thermal receiver, the lower the range of integration temperature, the more importance the effect of sunshine quality plays. However, in terms of the discharge efficiency of thermocline, the influence of temperature range is quite small.

(5)For the whole year operation, the annual solar power efficiency of superheat scheme is about 2.74% higher than that of the evaporation scheme, but the solar part of the latter scheme can work for longer time.

Acknowledgment

The financial supports for this research project from the National Natural Science Foundation of China (No.U1361108), the national "973 Program" of China (No. 2015CB251503) and the 111 Project (B12034) are gratefully acknowledged.

References

[1] The International Energy Agency (IEA). Concentrating Solar Power Roadmap; 2010

[2] Mills D. Advances in solar thermal electricity technology. Sol Energy 2004;76:19–31.

[3] Behar O, Khellaf A, Mohammedi K. A review of studies on central receiver solar thermal power plants. Renew Sustain Energy Rev 2013;23:12–39.

[4] Zhang D. Ultra-supercritical coal power plants: materials, technologies and optimisation. Philadelphia: Woodhead Pub; 2013.

[5] Yang H, Pollitt M. Incorporating both undesirable outputs and uncontrollable variables into DEA: The performance of Chinese coal-fired power plants. Eur J Oper Res 2009;197:1095–105.

[6] Zoschak RJ, Wu SF. Studies of the direct input of solar energy to a fossil-fueled central station steam power plant. Sol Energy 1975;17:297–305.

[8] Suresh MVJJ, Reddy KS, Kolar AK. 4-E (Energy, Exergy, Environment, and Economic) analysis of solar thermal aided coal-fired power plants. Energy Sustain Dev 2010;14:267–79.

[7] Popov D. An option for solar thermal repowering of fossil fuel fired power plants. Sol Energy 2011;85:344–9.

[9] Yang Y, Cui Y, Hou H, Guo X, Yang Z, Wang N. Research on solar aided coal-fired power generation system and performance analysis. Sci China Ser E TechnolSci 2008;51:1211–21.

[10] Yang Y, Yan Q, Zhai R, Kouzani A, Hu E. An efficient way to use medium-or-low temperature solar heat for power generation – integration into conventional power plant. ApplThermEng 2011;31:157–62.

[11] Hou H, Yang Y, Hu E, Song J, Dong C, Mao J. Evaluation of solar aided biomass power generation systems with parabolic trough field. Sci China TechnolSci 2011;54:1–7.

[12] Hou H, Wu J, Yang Y, Hu E, Chen S. Performance of a solar aided power plant in fuel saving mode. Appl Energy 2015;160: 873–81.

[13] Hou H, Yu Z, Yang Y, Chen S, Luo N, Wu J. Performance evaluation of solar aided feedwater heating of coal-fired power generation (SAFHCPG) system under different operating conditions. Appl Energy 2013;112:710–8.

[14] Peng S, Hong H, Wang Y, Wang Z, Jin H. Off-design thermodynamic performances on typical days of a 330MW solar aided coal-fired power plant in China. Appl Energy 2014;130:500–9.

[15] Cekirge HM, Elhassan A. A Comparison of Solar Power Systems (CSP): Solar Tower (ST) Systems versus Parabolic Trough (PT) Systems 2 . Comparison of Solar Tower (ST) and 2015;3:29–36.

[16] Spelling J, Favrat D, Martin A, Augsburger G. Thermoeconomic optimization of a combined-cycle solar tower power plant. Energy 2012;41:113–20.

[17] Zhang M, Yang L, Xu C, Du X. An efficient code to optimize the heliostat field and

comparisons between the biomimetic spiral and staggered layout. Renew Energy 2016;87:720–30.

[18] Patnode AM. Simulation and performance evaluation of parabolic trough solar power plants. MSME Thesis. University of Wisconsin-Madison, 2006.

[19] Pacheco JE, Showalter SK, Kolb WJ. Development of a Molten-Salt Thermocline Thermal Storage System for Parabolic Trough Plants. J Sol Energy Eng 2002;124:153.

[20] Xu C, Wang Z, He Y, Li X, Bai F. Sensitivity analysis of the numerical study on the thermal performance of a packed-bed molten salt thermocline thermal storage system. Appl Energy 2012;92:65–75.

[21] Bradshaw RW, Dawson DB, Rosa WDl, Gilbert R, Goods SH, Hale MJ, et al. Reilly HE, Showalter SK, Vant-Hull LL. Final test and evaluation results from the solar two project. In: Pacheco JE, editor. Report SAND2002e0120. Sandia National Laboratories; 2002.

[22] Ju X, Xu C, Wei G, Du X, Yang Y. A novel hybrid storage system integrating a packed-bed thermocline tank and a two-tank storage system for concentrating solar power (CSP) plants. ApplThermEng 2015;92:24–31.

[23] Crespo L, Ramos F, Martinez F. Questions and answers on solar central receiver plant design by NSPOC. In: Proceedings of the SolarPACES 2011 Conference, Granada; 2011.

[24] Yao Z, Wang Z, Lu Z, Wei X. Modeling and simulation of the pioneer 1MW solar thermal central receiver system in China. Renew Energy 2009;34:2437–46.

[25] Harris JA, Lenz TG. Thermal performance of solar concentrator/cavity receiver systems. Sol Energy 1985;34:135–42.

[26] Osuna, R., Fernandez, V., Romero, M., Blanco M. PS10: A 10 MW solar tower power plant for southern Spain. Proc. 10th SolarPACES Int. Symp. “Solar Therm. 2000,” Sydney,Australia: 2010, p. 13–8.

[27] Li X, Kong W, Wang Z, Chang C, Bai F. Thermal model and thermodynamic performance of molten salt cavity receiver. Renew Energy 2010;35:981–8.

[28] CHE DF. Boilers: theory, design and operation. Xi'an Jiaotong University Press; 2008.

[29] Strasser MN, Selvam RP. A cost and performance comparison of packed bed and structured thermocline thermal energy storage systems. Sol Energy 2014;108:390–402.

[30] Solar thermocline storage systems: preliminary design study. EPRI, Palo Alto, CA; 2010. p. 1019581

[31] Flueckiger SM, Iverson BD, Garimella S V., Pacheco JE. System-level simulation of a solar power tower plant with thermocline thermal energy storage. Appl Energy 2014;113:86–96.

[32] Lienhard JH, A Heat Transfer Textbook, Phlogiston Press, Cambridge, Massachusetts, U.S.A; 2002.

[33] Xiao P, Guo L, Zhang X. Investigations on heat transfer characteristic of molten salt flow in helical annular duct. ApplThermEng 2014:1–11.

[34] Lu J, He S, Ding J, Yang J, Liang J. Convective heat transfer of high temperature molten salt in a vertical annular duct with cooled wall. ApplThermEng 2014:6–11.

[35] Mokry S, Pioro I, Farah A, King K, Gupta S, Peiman W, et al. Development of supercritical water heat-transfer correlation for vertical bare tubes. NuclEng Des 2011;241:1126–36.

[36] Yang Z, Garimella S V. Thermal analysis of solar thermal energy storage in a molten-salt thermocline. Sol Energy 2010;84:974–85.

[37] Blair N, Mehos M, Christensen C, Janzou S. Solar advisor model user guide for version 2.0. National Renewable Energy Laboratory; 2008.

[38] Collado FJ, Guallar J. A review of optimized design layouts for solar power tower plants with campo code. Renew Sustain Energy Rev 2013;20:142–54.

Table captions

Table 1. The operation details of two integration schemes.

Table 2. Annual performance of integration systems in Scheme I.

Table 3.Results of comparisons between Scheme I and Scheme II.

Figure captions

Fig. 1. Schematic diagram of the whole system combining SPT and coal-fired power generating unit. (a) Solar energy and coal dual heat source boiler. (b) Solar tower heat aided coal-fired power generation.

Fig. 2. Schematic diagram of the heat exchanger in Scheme II

Fig. 3. The logic flow chart of whole system

Fig. 4. Three typical annual DNI distributionsof the typical meteorological year .(a) Original distribution. (b) expelling DNI below 15˚elevation.

Fig. 5. Variation of $\Delta B_{std}$and η_{sol} in one year with different storage volume. (a) 3h storage volume. (b) 4h storage volume. (c) 5h storage volume.

Fig. 6 Discard thermal energy during the whole year operation of Scheme I.

Fig. 7 Variation of $\eta_{TPG}$and $\eta_{discharge}$ in one year under different storage volume. (a) High DNI. (b) Medium DNI. (c) Low DNI.

Fig. 8 Comparisons of temperature profiles and heat transfer coefficient when Re number is 0.1, 1 and 1.(a) Temperature profiles and average temperature difference between salt and fillers. (b) Conductivity and heat transfer coefficient.

Fig. 9. Variations of ΔB_{std} and η_{sol}in one year under different DNI with 3h TES.

Fig. 10 Variations ofη_{TPG} and $\eta_{discharge}$in one year with TESvolume under medium DNI.